UNCOOLED IR PHOTON DETECTION USING MEMS MICRO-STRUCTURES

August 1998

P.G. Datskos and S. Rajic
Oak Ridge National Laboratory
P.O. Box 2009, MS-8039
Oak Ridge, TN 37831-8039

ABSTRACT

Generation of free charge carriers in a semiconductor gives rise to mechanical stress. Photo-induced stress phenomena in MEMS micro-structures can be used in the room temperature detection of infrared photons. Choice of the appropriate semiconductor material for the MEMS micro-structure the determines the cutoff wavelength of the uncooled infrared photon detector. We have measured the deflection of silicon and indium antimonide micro-structures resulting from a photo-induced stress. The excess charge carriers responsible for the photo-induced stress, were produced via photon irradiation from both a diode laser and a black body source. In the case of Si, the photo-induced stress is of opposite direction and about four times larger than the thermal stress. For indium antimonide the direction of stress is the same as due to thermal effects. The photo induced stress can be distinguished from the thermal stress based on the cut-off wavelength, response speed, and perhaps the direction of the microstructure deflection.

INTRODUCTION

The photo-generation of free charge carriers (electrons and holes) in a semiconductor, results in the development of a local mechanical stress [1]. This photo-induced stress will cause an expansion, or contraction, of the lattice similar to thermal excitation.

For a semiconductor with a bandgap energy ϵ_g, the change in total surface stress due to photo-generated excess charge carriers, Δn, and changes in temperature, ΔT, will be the sum of the photo-induced stress, Δs_{pi}, and thermal stress, Δs_{th}, given by [1-3],

$$\Delta s = \Delta s_{pi} + \Delta s_{th} = \left(\frac{1}{3} \frac{d\varepsilon_g}{dP} \Delta n \right) E + \alpha \Delta T E \qquad \textbf{(1)}$$

where, $d\epsilon_g/dP$ is the pressure dependence of the bandgap energy, α is the thermal expansion coefficient, and E is the Young's modulus. Since $d\epsilon_g/dP$ can be either positive or negative there can

REPORT DOCUMENTATION PAGE

Form Approved OMB No. 0704-0188

1. REPORT DATE (DD-MM-YYYY)	2. REPORT TYPE	3. DATES COVERED (FROM - TO)
01-08-1998	Conference Proceedings	xx-xx-1998 to xx-xx-1998

4. TITLE AND SUBTITLE
Uncooled IR Photon Detection Using MEMS Micro-Structures
Unclassified

5a. CONTRACT NUMBER
5b. GRANT NUMBER
5c. PROGRAM ELEMENT NUMBER

6. AUTHOR(S)
Datskos, P. G. ;
Rajic, S. ;

5d. PROJECT NUMBER
5e. TASK NUMBER
5f. WORK UNIT NUMBER

7. PERFORMING ORGANIZATION NAME AND ADDRESS
Oak Ridge National Laboratory
P.O. Box 2009, MS-8039
Oak Ridge, TN37831-8039

8. PERFORMING ORGANIZATION REPORT NUMBER

9. SPONSORING/MONITORING AGENCY NAME AND ADDRESS
Director, CECOM RDEC
Night Vision and electronic Sensors Directorate, Security Team
10221 Burbeck Road
Ft. Belvoir, VA22060-5806

10. SPONSOR/MONITOR'S ACRONYM(S)
11. SPONSOR/MONITOR'S REPORT NUMBER(S)

12. DISTRIBUTION/AVAILABILITY STATEMENT
APUBLIC RELEASE
,

13. SUPPLEMENTARY NOTES
See Also ADM201041, 1998 IRIS Proceedings on CD-ROM.

14. ABSTRACT
Generation of free charge carriers in a semiconductor gives rise to mechanical stress. Photoinduced stress phenomena in MEMS micro-structures can be used in the room temperature detection of infrared photons. Choice of the appropriate semiconductor material for the MEMS micro-structure the determines the cutoff wavelength of the uncooled infrared photon detector. We have measured the deflection of silicon and indium antimonide microstructures resulting from a photo-induced stress. The excess charge carriers responsible for the photo-induced stress, were produced via photon irradiation from both a diode laser and a black body source. In the case of Si, the photo-induced stress is of opposite direction and about four times larger than the thermal stress. For indium antimonide the direction of stress is the same as due to thermal effects. The photo induced stress can be distinguished from the thermal stress based on the cut-off wavelength, response speed, and perhaps the direction of the microstructure deflection.

15. SUBJECT TERMS

16. SECURITY CLASSIFICATION OF:			17. LIMITATION OF ABSTRACT	18. NUMBER OF PAGES	19. NAME OF RESPONSIBLE PERSON
a. REPORT	b. ABSTRACT	c. THIS PAGE	Public Release	7	Fenster, Lynn lfenster@dtic.mil
Unclassified	Unclassified	Unclassified			19b. TELEPHONE NUMBER International Area Code Area Code Telephone Number 703767-9007 DSN 427-9007

be a competing effect between the photo-induced and thermal stress. For example, when $d\epsilon_g/dP$ is negative, the photo-induced stress is of opposite sign than that of the thermal stress which will tend to make the semiconductor crystal contract. On the other hand when $d\epsilon_g/dP$ is positive, the photo-induced stress will tend to make the semiconductor crystal expand.

Assuming a semiconductor cantilever of length l, width w, and thickness t, the maximum displacement z_{max} due to photo-induced and thermal stresses is given by [4]

$$z_{max} \approx \frac{(1-\upsilon)\, l^2}{t} \frac{d\varepsilon_g}{dP} \Delta n + \frac{3(1-\upsilon)\, l^2}{t} \alpha \Delta T \qquad \textbf{(2)}$$

where υ is the Poisson's ratio. An absorbed power, Φ_e^{abs}, of photons with wavelength $\lambda < \lambda_c$ ($= h c / \epsilon_g$) will produce a number density of excess charge carriers, Δn, given by [2]

$$\Delta n = \eta \frac{\lambda}{hc} \frac{\tau_L}{l w t} \Phi_e^{abs} \qquad \textbf{(3)}$$

where η is the quantum efficiency, h is Planck's constant, c is the speed of light, and τ_L is the lifetime of the carriers in the semiconductor. The maximum displacement z_{max} due to photo-generated carrier scan then be written as [2]

$$z_{max} \approx \frac{(1-\upsilon)\, l^2}{t} \left(\eta \frac{\lambda}{hc} \frac{d\varepsilon_g}{dP} \frac{1}{l w t} + \frac{3\alpha}{m c_p} \right) \tau_L \Phi_e \qquad \textbf{(4)}$$

Since the charge carriers can be generated in a very short time the photo-induced stress can manifest itself much faster than thermal stress. Of course, the overall change in z_{max} will depend on the physical and mechanical properties of the semiconductor. From Eqn (4) we can estimate the relative contribution of the photo-induced stress and thermal stress to the bending of Si (ϵ_g =1.12 eV [5]) microcantilevers such as the one used in the present studies having length l = 100 μm, thickness t = 0.5 μm, and width w=20 μm. The amount of photon energy needed to raise the temperature of a mass of Si equal to 2.3×10^{-9} g by 10^{-5} K is $\Phi_e^{abs}\, \tau_d = (N h\nu = c_p m \Delta T =) 1.62\times10^{-14}$ J where c_p for Si is 0.702 $Jg^{-1}K^{-1}$. If the photon wavelength is λ= 1.1 μm then 8.94×10^4 photons will be required. Therefore, the bending due to thermal stress is $z_{max}^{th} = 1.39\times10^{-10}$ cm. In order to estimate the bending due to the photo-induced stress we assume the quantum efficiency η=1 and that the charge carriers are uniformly distributed. Then, the carrier number density is $\Delta n = 8.946\times10^{13}$ cm^{-3}. Using $d\epsilon_g/dP = -2.9\times10^{-24}$ cm^3 for Si [6] we get $z_{max}^{pi} = 5.19\times10^{-10}$ cm which is about 3.7 times larger than the deflection due to thermal stress for the same power. Applying Eqn (4) to indium antimonide results in more than an order-of-magnitude greater deflection response (z_{max}) due to photo induced effects compared to thermal excitation alone.

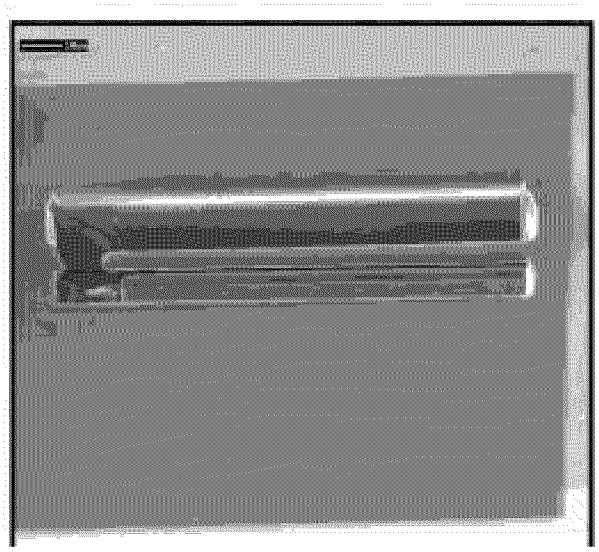

Figure 1. Silicon (Si) microcantilever used to generate initial feasibility results.

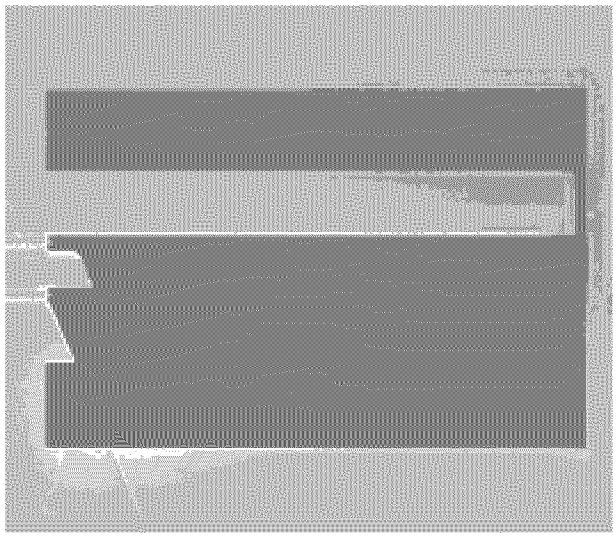

Figure 2. Indium Antimonide (InSb) bulk material microcantilever.

EXPERIMENTAL CONFIGURATION

The bending of microcantilevers can be measured with high sensitivity using detection techniques commonly used in atomic force microscopy (AFM) [7]. For example, Hansma [8] and Binnig [9] have demonstrated that changes in cantilever bending of 5×10^{-12} m can be measured. More recently even smaller microcantilever deflections were measured with a resolution of ~0.4×10^{-12} m [10]. We have performed studies on the effect of photo-induced stress and thermal stress on three types of micro-devices. Initial studies were performed on silicon microcantilevers with dimensions of l = 100 μm, w = 20 μm, and t = 0.5 μm with a 30 nm Al layer deposited on one side, shown in Fig. 1. Next, bulk indium antimonide microcantilevers were investigated with dimensions of l = 500 μm, w = 50 μm, and t = 3 μm, as shown in Fig. 2. Finally, a more representative ~ 50 μm x 50 μm detector element was fabricated that was gold coated with a barrier of SiN_x between the 500 nm of indium antimonide and 50 nm of gold as shown in Fig. 3. The bending of such microcantilevers can readily be determined by a number of means, including optical, capacitive, piezoresistive, and electron tunneling. In the present studies we used an optical readout technique for observing the microcantilever bending. The experimental setup used is shown schematically in Fig. 4. The location of a probe laser beam (reflected off the tip of the microcantilever) is detected using a position sensitive photodiode in which

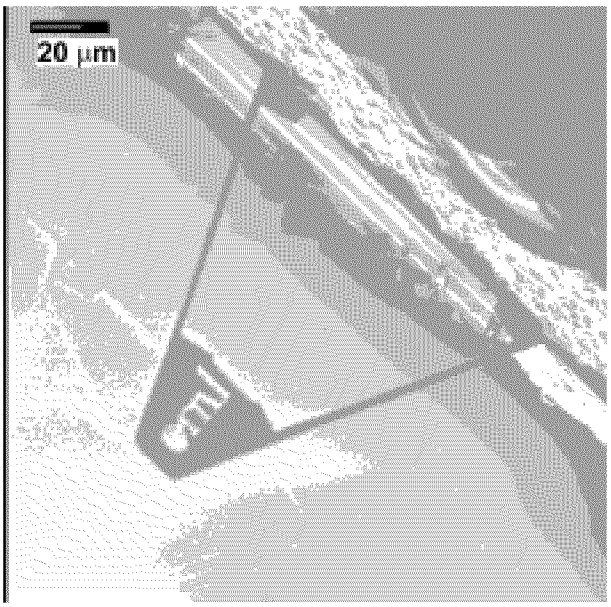

Figure 3. Au/SiN_x/InSb microcantilever in an approximately 2 mil active area configuration.

the bending of the microcantilever depends linearly on the current output of the photodiode. A narrow bandpass optical filter is placed in front of the photodiode allowing the probe laser beam to be detected while preventing other wavelengths from reaching the photodiode.

RESULTS

The microcantilever was exposed to near infrared photons from a diode laser with wavelength λ=780 nm and using a mechanical chopper, the infrared radiation was modulated at a frequency of 1000 Hz. In Fig. 5 we show the temporal response of the Si microcantilever (curve a) to the modulator signal (b). The absorbed optical power was 3.9 nW and was calculated using $\Phi_e^{abs} = \alpha_{abs}\, \Phi_e^{inc}\, A_{cant} / A_{spot}$, where α_{abs} ($\approx$ 0.95) is the absorptivity of Si at 780 nm, A_{cant} is the cantilever area and A_{spot} (= 1.53 mm^2) is the area of the focused laser beam at the plane of the microcantilever. The observed bending is attributed to the fact that the irradiated side (Si part) of the microcantilever *contracts* due to photo-induced stress while the Al layer of the microcantilever will tend to *expand*. Because of the bimaterial nature of the microcantilever, after a steady state condition is reached the micro-structure will remain bent while exposed to photons. As it can be seen from curve (a) in Fig. 5, the Si microcantilever responds rapidly to incoming photons that generate charge carriers which, in turn, cause a measurable mechanical bending. In these experiments, photons continued to impinge on the detector surface for ~ 5×10^{-4} s, while the bending reached its maximum value in ~ 1×10^{-4} s. The time that the microcantilever reached its maximum bending corresponds nicely to the lifetime of photo-generated "free" charge carriers in Si.

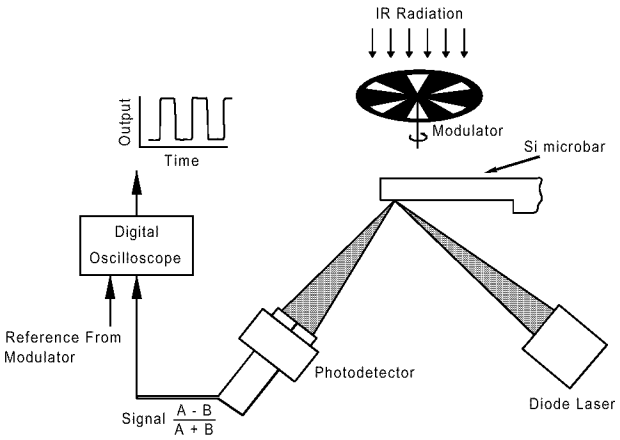

Figure 4. Schematic diagram of the experimental setup used in the present studies.

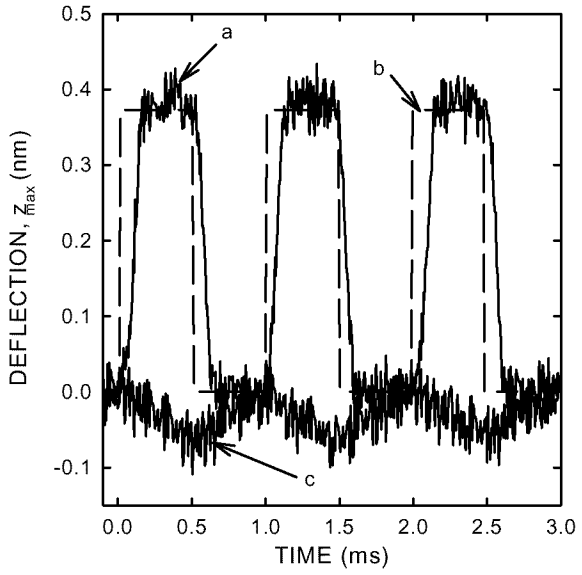

Figure 5. Deflection of a Si microcantilever as a function of time. (a) photo-generated charge carriers deflection (λ=780 nm). (b) dashed curve represents modulator signal. (c) deflection due to thermal effects (λ=1300 nm).

In contrast to the photo-induced effects, thermal effects have been found to play a role in a slower time scale and have a time constant > 10^{-3} s [11-13]. In order to determine the effect of the thermal stress under our experimental conditions, we

illuminated the Si microcantilever using photons with λ=1300 nm. Since Si is transparent to these photons, we had deposited a thin aluminum coating of 30 nm along one side of the Si microcantilever. The absorbed power was estimated using $\Phi_e^{abs} = \alpha_{abs}\ \Phi_e^{inc}\ A_{Al} / A_{spot}$ where $\alpha_{abs} = 0.01$ is the absorptivity of Al and A_{Al} ($= 2\times10^{-5}$ cm^2) is 3the area of the Al layer. We modulated the infrared radiation for the 1300 nm diode laser at a frequency of 1000 Hz. In Fig. 5 curve (c) we plotted the measured microcantilever response as a function of time due to absorption of 1300 nm photons for an absorbed power of 2 nW. Of course, the observed microcantilever bending depends on the difference between the coefficient of thermal expansion of Si and Al (bimaterial effect). Since Si is transparent to photons with λ= 1300 nm the Al layer heats up and the thermal stress causes the Al to expand forcing the microcantilever to bend in a direction opposite to that shown in curve (a) which is due to the photo-induced stress. From curve (c) in Fig. 5 it can be seen that for 1300 nm photons and 1000 Hz modulation frequency, the observed thermally-induced bending of the microcantilever is smaller (over 2 times after correcting for the absorbed power) compared to the photo-induced bending [curve (a)] . Furthermore, the microcantilever response to the photo-induced stress [curve (a) in Fig. 5] is much faster than the response due to thermal effects [curve (c) in Fig. 5].

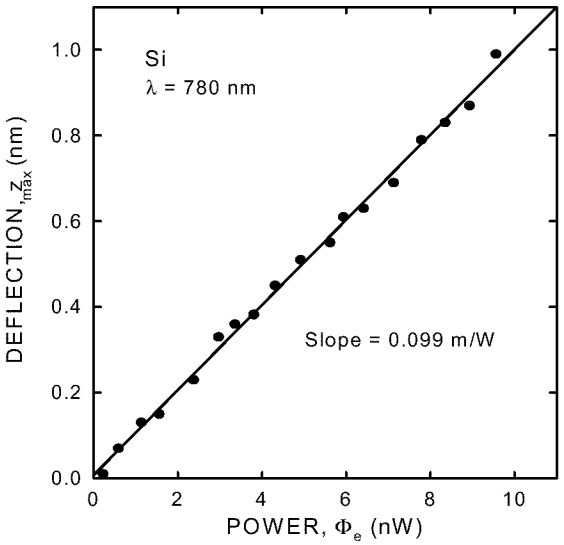

Figure 6. Deflection of a Si microcantilever as a function of absorbed power due to photo-generated charge carrier (λ=780 nm).

Since $d\epsilon_g/dP$ is negative for Si [6], it is straightforward to separate the photo-induced from the thermal effects in Si by simply observing the direction of bending indicated by the phase shift of the signal waveform with respect to the reference signal. When photons with energies above the bandgap are used to irradiate the Si microcantilever, Si contracts and deflects in one direction [curve (a) in Fig. 5]. However, when photons with energies below the bandgap are used, both Al and Si will tend to expand and the microcantilever will deflect in the opposite direction [curve (c) in Fig. 5].

We measured the microcantilever bending due to photo-induced stress as a function of absorbed power. In Fig. 6 we plotted the measured bending of a Si microcantilever as a function of absorbed power using a diode laser with λ=780 nm. The microcantilever deflection was primarily due to photo-induced stress and was found to increase linearly with increasing power with a deflection sensitivity of 0.099 m/W. We also illuminated the bulk indium antimonide microcantilever shown earlier in Fig.2 with infrared photons from a black body source through a mechanical chopper and observed the response. Since this was an uncoated bulk material device, the signal was transient in nature. However, since a relatively rapid chopping frequency was used we were able to measure the response of the device as can be seen from Fig. 7. Since this was a large device with appreciable thermal mass, the less than 2 ms rise time was encouraging since thermo-mechanical deflection for

this device was predicted to be substantially slower. For indium antimonide both the photo-induced and thermal stresses will deflect the device in the same direction. However, from Fig.2 it can be seen that this device is very well heat sunk compared to conventional thermally isolated uncooled detectors.

The device shown in Fig.2 represents an initial feasibility indium antimonide micro-devices intended to quickly demonstrate the photo-induced deflection effect in an infrared material. The most recent devices fabricated, shown in Fig. 3, use a Au/SiN_x/InSb [14] structure and more closely represent a viable detector element with an approximately 50 μm×50 μm absorbing area. This device has been optimized for sensitivity by making the structure more pliable with thinning and narrowing of the supporting legs. However, this step also increases thermal isolation which may produce an undesirable competing thermal effect in this type of detector. Studies are underway to measure frequency response to verify the dominant driving mechanism for this device architecture.

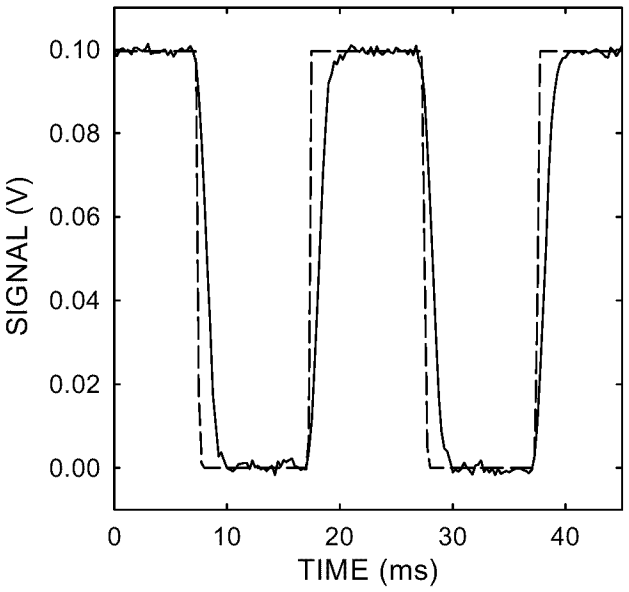

Figure 7. Response of InSb bulk material microcantilever.

CONCLUSIONS

We have demonstrated that photo-induced stress phenomena in MEMS micro-structures can be used in uncooled infrared photon detection. Choice of the appropriate semiconductor material for the MEMS micro-structure the determines the cutoff wavelength of the uncooled infrared photon detector. Our present studies demonstrate that irradiating microcantilevers with photons having energies above the bandgap results in a photo-induced mechanical stress. When the photon energy is below the bandgap, thermal effects are observed. The photo-induced stress was found to depend linearly on the input optical power and exhibit a fast response. Since all of our studies were performed at room temperature, such a mechanism may eventually be used as an efficient uncooled micro-mechanical infrared quantum detector.

ACKNOWLEDGMENT

This research was conducted at the Oak Ridge National Laboratory and supported by DARPA under contract No.1868-HH01-X1. The Oak Ridge National Laboratory is managed by Lockheed Martin Energy Research Corporation for the Department of Energy.

REFERENCES

[1] T. Figielski, "Photostriction Effect in Germanium," *Phys. Status Solidi* **1**, 306 (1961).

[2] P. G. Datskos, S. Rajic, I. Datskou, and C. M. Egert, "Novel Photon Detection Based on Electronically-Induced Stress in Silicon," *IR Detectors and Focal Plane Arrays V, SPIE* **3978** (1998).

[3] P. G. Datskos, S. Rajic, and I. Datskou, "Photo-Induced Stress in Silicon Microcantilevers," *Appl. Phys. Lett.* (in press).

[4] F. J. von Preissig, "Applicability of Classical Curvature-Stress Relation for Thin Films on Plate Substrates," *J. Appl. Phys.* **66**, 4262 (1989).

[5] E. L. Dereniak and G. D. Boreman, *Infrared Detectors and Systems*. New York: Wiley and Sons, 1996.

[6] R. C. Weast, *Handbook of Chemistry and Physics*, 59th ed. Florida: CRC, 1972.

[7] D. Sarid, *Scanning Force Microscopy*. New York: Oxford University Press, 1991.

[8] J. H. Hoh, J. P. Cleveland, J.-P. Prater, and P. K. Hansma, "Quantized Adhesion Detected with Atomic Force Microscope," *J. Am. Chem. Soc.* **114**, 4917 (1992).

[9] F. Ohnesorge and G. Binning, "True Atomic Resolution by Atomic Force Microscopy Through Repulsive and Attractive Forces," *Science* **260**, 1451 (1993).

[10] J. Lai, T. Perazzo, Z. Shi, and A. Majumdar, "Optimization and Performance of High-Resolution Micro-Optomechanical Thermal Sensors," *Sensors and Actuators* **58**, 113 (1997).

[11] P. G. Datskos, P. I. Oden, T. Thundat, E. A. Wachter, R. J. Warmack, and S. R. Hunter, "Remote Infrared Detection Using Piezoresistive Microcantilevers," *Appl. Phys. Lett.* **69**, 2986 (1996).

[12] P. I. Oden, E.A. Wachter, P.G. Datskos, T. Thundat, and R.J. Warmack, "Optical and Infrared Detection Using Microcantilevers," *SPIE - Infrared Technology XXII* **2744**, 345 (1996).

[13] J. R. Barnes, R. J. Stephenson, C. N. Woodburn, S. J. O'Shea, M. E. Welland, T. Rayment, J. K. Gimzewski, and C. Gerber, "Femtojoule Calorimeter Using Micromechanical Sensors," *Rev. Sci. Instrum.* **65**, 3793 (1994).

[14] J. W. Buttrey, "Small Magnetic Field Mapping Probes of Thin Semiconducting Films," *Rev. Sci. Instrum.* **30**, 815 (1959).